Impact on the Spatial Resolution Performance of a Monolithic Crystal PET Detector Due to Different Sensor Parameters

Xiaoli Li, *Student Member, IEEE*, Cate Lockhart, Tom K. Lewellen, *Fellow, IEEE,* and Robert S. Miyaoka, *Member, IEEE*

***Abstract*– The performance characteristics of a monolithic crystal PET detector utilizing a novel sensor on the entrance surface (SES) design is reported. To facilitate this design, we propose to utilize a 2D silicon photomultiplier (SiPM) array device. SiPMs are a form of Geiger-Muller mode avalanche photodiodes (GMAPD) that can provide signal gain similar to a photomultiplier tube (PMT). Since these devices are still under active development, their performance parameters are changing. Using a multi-step simulation process, we investigated how different SiPM parameters affect the performance of a monolithic crystal PET detector. These parameters include gain variability between different channels; gain instability; and dark count noise. The detector simulated was a 49.6 mm by 49.6 mm by 15 mm LYSO crystal detector readout by a 16 by 16 array of 2.8 mm by 2.8 mm SiPM elements. To reduce the number of signal channels that need to be collected, the detector utilizes row-column summing. A statistics based positioning method is used for event positioning and depth of interaction (DOI) decoding. Of the variables investigated, the dark count noise had the largest impact on the intrinsic spatial resolution. Gain differences of 5-10% between detector calibration and detector testing had a modest impact on the intrinsic spatial resolution performance and led to a slight bias in positioning. There was no measurable difference with a gain variability of up to 25% between the individual SiPM channels. Based upon these results we are planning to cool our detectors below room temperature to reduce dark count noise and to actively control the temperature of the SiPMs to reduce drifts in gain over time.**

I. Introduction

We have previously reported on a high resolution, monolithic crystal PET detector design that provides depth of interaction (DOI) positioning within the crystal [1]. This design utilizes a novel sensor on the entrance surface (SES) design combined with a maximum likelihood positioning algorithm. It provides outstanding X, Y and DOI resolution and allows the detector to provide nearly the same intrinsic spatial resolution for normally and 45º incident photon fluxes.

One of the keys to the SES design is the development of SiPMs [2,3]. SiPMs provide very high proportional signal gain, have potentially very fast timing, and can be fabricated in user specified geometries. In our application, we are taking advantage of the fact that SiPMs are very thin and can be placed on the entrance surface of the crystal without having a significant attenuation effect. In addition, the SiPMs can be operated in high magnetic fields, which enables PET/MR multimodal imaging.

Since SiPM is a new technology that is under active development, their performance parameters are still changing. In this paper, how the SiPM parameters affect the performance of the PET detector is investigated.

II. Detector Design and Methods

A. SiPM performance parameters

As the photosensor for PET detectors, the parameters of SiPMs have a significant impact on the spatial resolution performance of our monolithic crystal PET detector.

One of the most important parameters for SiPMs is their gain uniformity between different channels. For a monolithic crystal PET detector, one crystal is readout by an array of SiPM elements. SiPM arrays with ~25% gain variation between different channels have been manufactured [SensL]. It is unclear how this gain variation might affect the performance of a PET detector. This is especially important in our design because to reduce the number of data readout channels, the SiPM arrays were row-column summed. This reduced the number of signal channels from 256 to 32 for a 16 by 16 SiPM array.

Another complication is that the SiPM gains may shift over time due to changes in the environment, such as temperature or power supply stability. Experiments by our group show that the gain shift can be as much as 8.5%/°C [4]. The gain shift might lead to positioning bias and degraded resolution.

Like most semiconductor devices, SiPMs are susceptible to thermal noise. Preliminary results by our group show that the dark count rate increases significantly with temperature [4]. The dark count rate due to thermally generated electrons may degrade the positioning resolution of a detector.

Manuscript received November 13, 2009. This work was supported in part by the NIH grants NIBIB EB001563 and EB002117, DOE grant DE-FG02-08ER64676 and Zecotek Photonics.

X. Li is with the University of Washington Department of Physics, Seattle, WA USA (phone: 206-543-0629; fax: 206-543-8356; e-mail: lixioli@u.washington.edu).

C. Lockhart is with the University of Washington Department of Pharmaceutics, Seattle, WA USA (e-mail: cmo4@u.washington.edu).

T. K. Lewellen is with the University of Washington Department of Radiology, Seattle, WA USA (e-mail: tkldog@u.washington.edu).

R. S. Miyaoka is with the University of Washington Department of Radiology, Seattle, WA USA (e-mail: rmiyaoka@u.washington.edu).

B. Statistics-based positioning (SBP) algorithm with DOI decoding

A statistics based positioning (SBP) algorithm is used to improve the detector positioning characteristics of the detector compared to standard or modified Anger positioning schemes [5]. Suppose, the distributions of observing signal outputs M = M_1, M_2… M_n for scintillation position x, are independent normal distributions with mean, $\mu_i(x)$, and standard deviation $\sigma_i(x)$.

The likelihood function for making any single observation m_i from distribution M_i given x is:

$$L[m_i \mid x] = \prod_{i=1}^{n} \frac{1}{\sigma_i(x)\sqrt{2\pi}} \exp\left(-\frac{(m_i - \mu_i(x))^2}{2\sigma_i^2(x)}\right) \quad (1)$$

The maximum likelihood estimator of the event position x is given by:

$$\hat{x} = \arg\min_x \left[\sum_i \frac{(m_i - \mu_i(x))^2}{2\sigma_i^2(x)} + \ln(\sigma_i(x))\right] \quad (2)$$

The SBP method requires that the light response function versus interaction location be characterized for the detector. Two SBP look-up tables (LUTs) corresponding to the mean and variance of the light probability density function (PDF) versus (X,Y) position are created during the calibration process.

To further improve the decoding performance of the detector, a maximum-likelihood (ML) clustering method is used to extract depth of interaction (DOI) information during the calibration of the detector module. [6] The DOI separation technique divides the calibration data into different DOI regions. LUTs are then created for each DOI region. The full set of DOI LUTs allows 3D positioning within our detector module. Our ML clustering technique has been used to extract up to 7 DOI regions from our 15 mm thick cMiCE detector. Based on the 7-depth DOI LUT, a third-order polynomial fit is applied to the mean and variance respectively for each (X,Y) position. Then, a 15-depth DOI LUT is generated from the fitting result.

The algorithm utilizes the fact that the light distribution pattern varies continuously and smoothly with DOI so scintillation events happening in similar DOI regions of the crystal will produce similar light distribution patterns. The 7-depth DOI LUT generation can be separated into five basic steps.

Step 1. For the training data at each position, the photosensor channel N receiving the maximum amount of light is located. The light histogram data for the maximum channel is separated into seven initial groups according to their pulse height in photosensor channel N. Group 1 consists of events within the highest one-seventh of the PDF histogram, which correspond to interactions occurring closest to the photosensors in the crystal. Group n (n=2 … 6) consists of events with the nth one-seventh highest section of the histogram. Group 7 consists of events comprising the lowest one-seventh of the PDF histogram, which correspond to interactions occurring in the crystal furthest from the photosensors. While the initial separation is based upon the pulse height of the signal in photosensor channel N, each event consists of signals from all 64 channels. In doing our depth separation, we use all the channels.

Step 2. For each set of data (i.e., groups 1 through 7), the mean $\mu(j)_i$ and standard deviation $\sigma(j)_i$ are generated, where i is the number of the photosensor channel and j is the group number.

Step 3. For each event, the likelihood ratios (LR) between different groups are calculated. Separation in LR can be used to tune the number of events falling in each group. After all the data has been sorted, iterate by going back to Step 2.

Step 4. After a stable separation is reached, the final mean and standard deviation are generated where they represent the light response LUTs for DOI regions 1 through 7, respectively.

Step 5. For each (X,Y) position, a third-order polynomial fit is applied to the seven DOI means and standard deviations, respectively. A 15-depth DOI LUT is generated from the fitting results.

The idea behind the initial grouping in step 1 is that the signal from channel N correlates with DOI, shown in figure 1. Based upon solid angle considerations, interactions near the photosensor window will have a larger amount of light collected by the photosensor channel directly under the interaction location than interactions further from the photosensor.

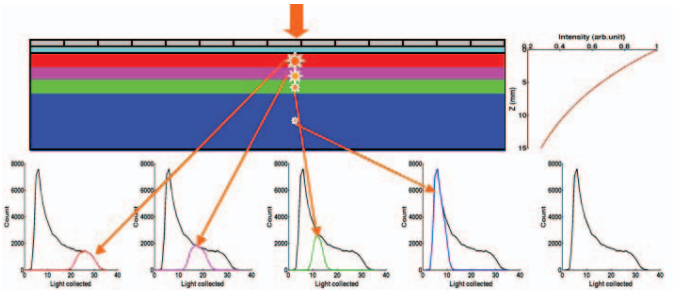

Fig. 1. Principle of ML clustering algorithm for DOI decoding.

C. Simulation program for look up table (LUT) generation and testing

We use simulation tools that we have previously integrated to investigate PET detector performance with different SiPM parameters. DETECT2000 [7,8] is used to determine the probability that a light photon generated at a specific position in the crystal is detected by a specific photosensor. GEANT [9] is used to track the gamma interactions (both Compton scattering and photoelectric) within the crystal. The non-proportionality of LYSO was also modeled according to tables reported by Rooney [10]. Finally, Poisson noise is added to the detected light signals. To test how non-uniform gains affect the detector performance, the number of light photons detected by the SiPM array is adjusted by a gain table with 25% non-uniformity. To test how gain shifts affect the detector performance, the gains for the testing data are shifted

-10+/-2% or -5+/-5% compared to the gains during detector calibration. Finally to test how dark count noise affects the detector performance, Poisson noise with mean value of 1, 2 and 3 was added to each SiPM channel. This corresponds to dark count rates of 6.67 MHz, 13.3 MHz and 20 MHz.

D. Detector setup

For this initial work, the crystal was modeled as a 49.6 mm by 49.6 mm by 15 mm slab of LYSO. Considering the symmetry of the detector, one eighth of the crystal was simulated to speed up the calibration and testing process. A 16 by 16 array of 2.8 mm by 2.8 mm SiPM elements with 3.1 mm center-to-center spacing was placed on the entrance surface of the crystal. The photon detection efficiency of the SiPM was set at 15%. Fifteen-depth DOI LUTs were built from photon fluxes perpendicular to the detector with FWHM of 0.6 mm. The testing events were simulated as having a point flux of normal incidence. The spacing between photon fluxes was 1.55 mm in X and Y. The effect of Compton scatter in the crystal was included for both the calibration and testing data. To reduce the number of processing channels the SiPM arrays were row-column summed. So event positioning was based upon signals from 32 channels.

III. RESULTS

Figure 2 illustrates the 2 dimensional FWHM contour plots illustrating the intrinsic spatial resolution using 15-depth SBP positioning for gain variability of 25%, dark count noise of 0 and 2, gain shift of -10+/-2% and -5+/-5%, and with no gain shift. As can be seen, adding dark count noise degrades the X/Y spatial resolution. And gain shifts for testing data comparing with the calibration data lead to X/Y positioning bias, especially at the edges of the crystal.

Table I summarizes the intrinsic resolution results calculated using a Gaussian fit to the data for 0 and 25% gain variation between different SiPM channels. As can be seen, the results with 25% gain variation and without gain variation are almost identical. Introducing 25% gain variability between different SiPM channels does not affect the detector performance.

Table II summarizes the intrinsic resolution results for varying gain shifts. The gain shifts lead to positioning bias and worse resolution. As expected, the effect is bigger for a shift of -10+/-2% than a shift of -5+/-5%.

Table III summarizes the intrinsic resolution results for varying dark count noise. The X/Y/DOI resolution becomes worse when increasing dark count noise, while the positioning bias does not increase much.

IV. DISCUSSION AND CONCLUSION

Among all the three SiPM parameters investigated here, the dark count noise has the largest impact on the spatial resolution performance. Therefore, cooling down the system is required to achieve optimal detector performance.

A gain variability of 25% doesn't affect the detector performance. Because the gain variability affects the calibration and testing data similarly, it can be compensated when using the SBP positioning algorithm.

When the gains for the testing data are negatively shifted compared to the gains for the calibration data, the testing events are bias towards the edge and bottom of the detector, this would introduce artifacts to reconstructed images. Since the gains of the SiPMs are very sensitive to temperature, the temperature of the system needs to remain constant during experiments.

In summary, based on the simulation study, we plan to cool and actively control the temperature of the SiPM array below room temperature during experiment to reduce the dark count rate and gain shifts due to temperature variations.

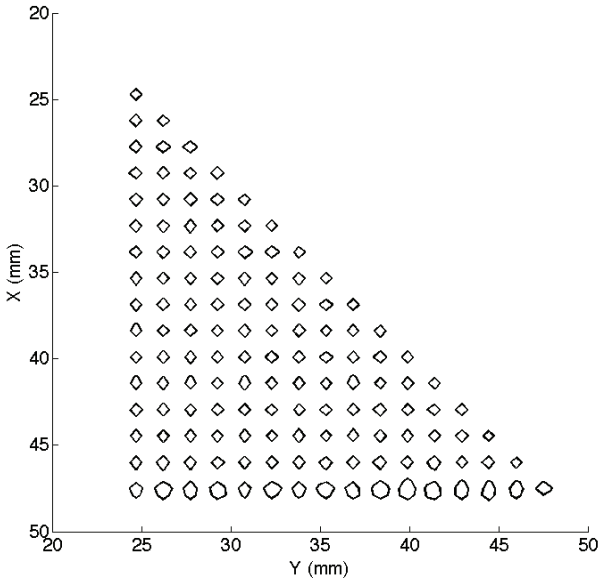

(a)

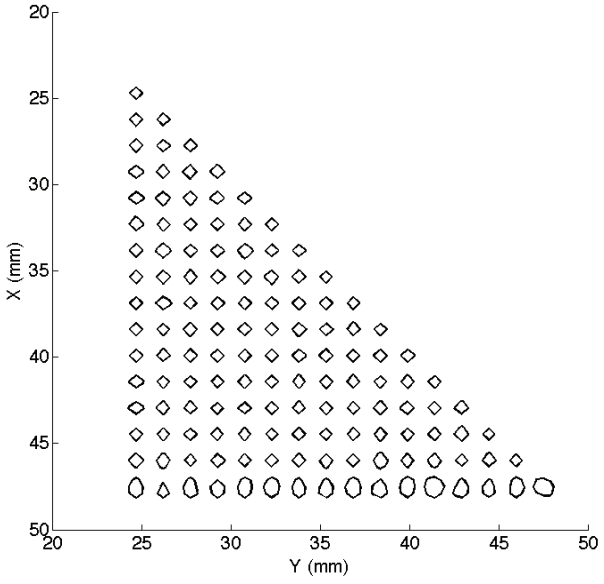

(b)

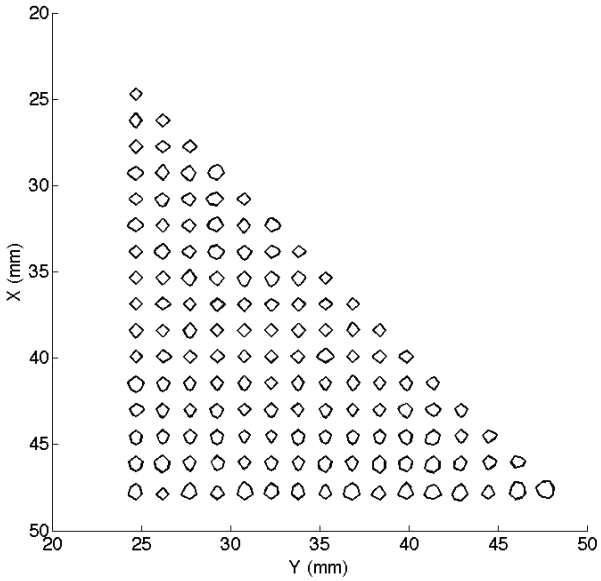

(c)

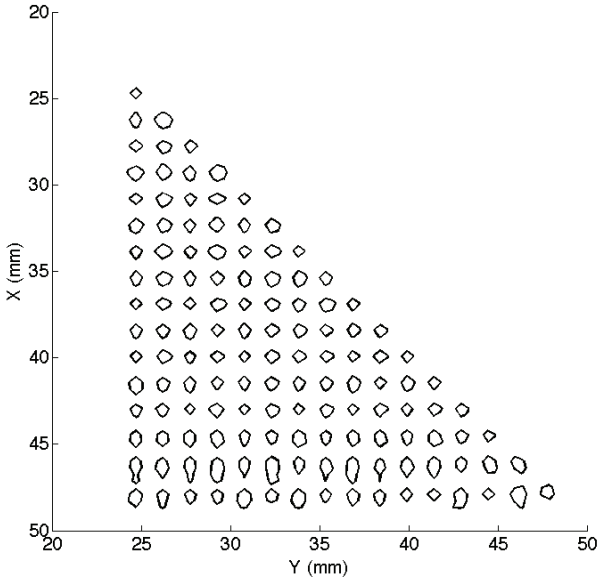

(d)

Fig. 2. 50% contour plots of SBP positioning using 15-depth DOI LUT for (a) gain variability of 25%, no dark count noise and no gain shift; (b) gain variability of 25%, dark count noise of 2 and no gain shift; (c) gain variability of 25%, dark count noise of 2 and -5+/-5% gain shift; (d) gain variability of 25%, dark count noise of 2 and -10+/-2% gain shift.

Table I. Varying gain variation between different channels, gain shift = 0, noise = 0

Gain var.	Dimension	Bias (mm)	FWHM (mm)
0	X/Y	0.00+/-0.03	0.73+/-0.09
	DOI	-0.03+/-0.14	1.66+/-0.14
25%	X/Y	0.00+/-0.03	0.73+/-0.09
	DOI	-0.03+/-0.14	1.66+/-0.16

Table II. Varying dark count noise, gain variation = 25%, gain shift = 0

Noise	Dimension	Bias (mm)	FWHM (mm)
0	X/Y	0.00+/-0.03	0.73+/-0.09
	DOI	-0.03+/-0.14	1.66+/-0.16
1	X/Y	0.00+/-0.03	0.77+/-0.08
	DOI	0.03+/-0.17	1.91+/-0.27
2	X/Y	0.01+/-0.03	0.82+/-0.09
	DOI	0.08+/-0.22	2.12+/-0.41
3	X/Y	0.01+/-0.03	0.86+/-0.09
	DOI	0.13+/-0.22	2.28+/-0.41

Table III. Varying gain shift between detector testing and calibration, gain variation = 25%, noise = 2

Gain shift	Dimension	Bias (mm)	FWHM (mm)
0	X/Y	0.01+/-0.03	0.82+/-0.09
	DOI	0.08+/-0.22	2.12+/-0.41
-5+/-5%	X/Y	0.03+/-0.07	0.82+/-0.09
	DOI	0.27+/-0.28	2.32+/-0.45
-10+/-2%	X/Y	0.10+/-0.14	0.83+/-0.20
	DOI	0.36+/-0.38	2.59+/-0.58

REFERENCES

[1] X. Li, C. Lockhart, T. K. Lewellen and R. S. Miyaoka, "A high resolution, monolithic crystal, PET/MRI detector with DOI positioning capability," *IEEE EMBS*, pp. 2287-2290, 2008.

[2] V. Saveliev and V. Golovin, "Silicon avalanche photodiodes on the base of metal-resistor-semiconductor (MRS) structures," *Nuclear Instruments & Methods in Physics Research Section a-Accelerators Spectrometers Detectors and Associated Equipment*, vol. 442, pp. 223-229, 2000.

[3] D. J. Herbert, V. Saveliev, N. Belcari, N. D'Ascenzo, A. Del Guerra, and A. Golovin, "First results of scintillator readout with silicon photomultiplier," *IEEE Transactions on Nuclear Science*, vol. 53, pp. 389-394, 2006.

[4] W. C. J. Hunter, R. S. Miyaoka, L. R. MacDonald and T. K. Lewellen, "Measured temperature dependence of scintillation camera signals readout by SiPMs," *IEEE NSS-MIC conference record*, 2009.

[5] J. Joung, R. S. Miyaoka, and T. K. Lewellen, "cMiCE: a high resolution animal PET using continuous LSO with a statistics based positioning scheme," *Nuclear Instruments & Methods in Physics Research Section a – Accelerators Spectrometers Detectors and Associated Equipment,* vol. 489, pp. 584-598, 2002

[6] T. Ling, T. K. Lewellen, and R. S. Miyaoka, "Depth of interaction decoding of a continuous crystal detector module," *Physics in Medicine and Biology,* vol. 52, pp. 2213-2228, 2007.

[7] G. Tsang, C. Moisan, and J. G. Rogers, "A simulation to model position encoding multicrystal PET detectors," *IEEE Transactions on Nuclear Science*, vol. 42, pp. 2236-2243, 1995.

[8] G. F. Knoll, T. F. Knoll, and T. M. Henderson, "Light Collection in Scintillation Detector Composites for Neutron Detection," *IEEE Transactions on Nuclear Science*, vol. 35, pp. 872-875, 1988.

[9] S. Agostinelli, et al., "GEANT4-a simulation toolkit," *Nuclear Instruments & Methods in Physics Research Section a-Accelerators Spectrometers Detectors and Associated Equipment*, vol. 506, pp. 250-303, 2003.

[10] B. D. Rooney and N. D. Valentine, "Scintillator light yield nonproportionality: Calculating photon response using measured electron response," *IEEE Transactions on Nuclear Science*, vol. 44, pp. 509-516, 1997.